Supplementary Information

Green synthesized Fe-Zn bimetallic nanoparticles alleviated Cadmium accumulation and enhanced plant growth in *Oryza sativa* L. cv (IR64)

S1. Materials and Methods:

S1.1. Analysis of photosynthetic parameters:

For estimation of chlorophyll a, chlorophyll b, total chlorophyll and carotenoid content, 50mg fresh leaves were finely chopped and the chlorophyll contents were extracted in 2ml of 80% acetone after overnight incubation. The absorbance was noted at 470, 646.8 and 663.2nm using a UV-Vis spectrophotometer (Shimazdu). The concentrations were calculated using the following equations and were expressed as µg g^{-1} FW [1]:

$C_a = 12.25A663.2–2.79A646.8$

$C_b = 21.5A646.8–5.1A663.2$

$C_{a+b} = 7.15\ A663.2 + 18.71A646.8$

$C_{x+c} = (1000A_{470} – 1.82C_a −85.02C_b)/198$

δ-Aminolevulinic acid (δ-ALA) content: δ-ALA is considered to be the precursor molecule of the tetrapyrrole compound chlorophyll which was quantified from fresh shoot tissue of 21days old seedlings. δ-ALA content was extracted by homogenising 100mg shoot with 0.1N TCA and centrifuged at 12,000rpm for 15mins under cold conditions [2]. The pH of the supernatant was adjusted to 4,5 by adding 50 µl 1M sodium acetate. The reaction mixture comprising of 300 µl supernatant and 42 µl acetylacetone was incubated in boiling water bath for 10mins. After incubation, 300 µl Ehlrich reagent was added which was followed up by 20 mins incubation in dark. The absorbance was recorded at 550nm and the δ-ALA content was expressed as mg g^{-1} FW.

Porphobilinogen (PBG) content: For PBG content estimation, 100mg plant tissue was extracted in 1ml 0.6M Tris-HCl buffer pH 8.2 containing 0.1M EDTA. Thereafter, centrifugation was performed and equal volume of supernatant as well as Ehlrich reagent was incubated for 15mins under dark conditions. The absorbance was noted at 553nm and the values were calculated using molar extinction coefficient ($\varepsilon = 6.1 \times 10^4$ L $mM^{-1}cm^{-1}$) [3,4]. PBG (µg/g) =

[226 × (A_{553})/MEC] × V/(1000 × W) where V is the volume of the extraction solution (mL), W is the weight of leaves (g), and MEC is the molar extinction coefficient (ε = 6.1 × 10^4 L $mM^{-1}cm^{-1}$). The PBG content was finally expressed as mg g^{-1} FW.

Hill Activity: Hill activity was evaluated using the protocol illustrated by Bauer and Senser, [5] in terms of DCPIP reduction in illuminated extract of fresh shoot tissue. 100mg shoot tissue was homogenised in 50mM potassium phosphate buffer pH 6.2 containing 0.4M sucrose and centrifuged at 1000g for 5mins. The supernatant was collected in fresh tube and the pellet was discarded which was followed up by re-centrifugation at 5000g for 15mins. Thereafter, the pellet was acquired and suspended in 1ml homogenisation buffer pH 6.2. The absorbance of final reaction mixture with 125 µl supernatant, 812.5 µl 50mM potassium phosphate buffer and 62.5 µl 0.03% DCPIP was immediately recorded at 610nm. This reaction mixture was further exposed to strong incandescence light till 3mins and the absorbance was again recorded at 610nm. Finally, Hill activity was represented as µM DCPIP reduced mg^{-1} chlorophyll h^{-1}.

Estimation of photosynthetic products: Total soluble sugar and starch content from fresh root and shoot tissue was determined by following the protocol outlined by Dubois *et al.* [6]. 100mg plant tissue was extracted in 1ml 80% ethanol and centrifuged after which the supernatant was collected for analysis of total soluble sugar, reducing sugar content and the pellet was reserved for starch content analysis. Subsequently, the pellet was dissolved in 1ml 52% perchloric acid and centrifuged at 2000rpm for 20mins. The supernatant was procured for starch content estimation. For soluble sugar estimation, the reaction mixture consisted of 25µl supernatant, 25 µl 5% phenol and 125 µl conc. H_2SO_4. The reaction mixture for starch content determination comprised of 37.5µl supernatant, 32.5µl H_20, 5 µl 5% phenol and 45µl conc. H_2SO_4. Both the reaction mixtures were incubated at 25-30ºC for 20mins and the absorbance was recorded in a Varioskan LUX (Thermo Scientific) multimode microplate reader at 490nm. The contents were calculated from a standard curve formulated using glucose and expressed as mg g^{-1} FW. The reaction mixture for reducing sugar comprised of equal volumes of supernatant and DNSA which was further incubated in boiling water bath for 5mins. Furthermore, the reaction mixture was allowed to cool down and the absorbance was noted down at 515nm [7]. The non-reducing sugar content was estimated by calculating the difference between total soluble sugar and reducing sugar contents.

S1.2. Analysis of morphological alterations in root tips as studied by SEM imaging:

The morphological changes of root tips and stomata of 21days old seedlings were visualised using Scanning Electron Microscope (SEM ZEISS EVO-MA 10; Carl Zeiss Pvt. Ltd., Oberkochen). Root tips from all treatment conditions were collected and dehydrated using gradient concentrations of ethanol (30, 50, 70, 80, 90, and 100%) up to 20mins and sputter-coated with Platinum for documentation under SEM. For visualisation of external morphology of stomata, leaf samples for all treatment set were cut into 0.5cm pieces following which they were subjected to similar treatment procedure as the root tip for visualisation [8].

S1.3. Determination of oxidative stress parameters:

ROS estimation: Total Reactive oxygen species (ROS) from root and shoot tissue was assessed following the protocol outlined by Jambunathan[9]. 100mg root and shoot tissue was homogenised with 1ml 10mM Tris-HCl Buffer pH (7.2) in cold conditions. Following centrifugation, the supernatant was collected and the final reaction mixture comprised of 1µl supernatant, 99 µl Tris-HCl Buffer, 1µl Dichlorodihydrofluorescein diacetate (H_2DCFDA). The readings were recorded at excitation and emission wavelength of 495 and 525nm respectively using a microplate reader.

For *in-situ* detection of ROS, root tips were incubated in 25µM DCFDA for 30 mins in room temperature under dark conditions and washed thoroughly in 1X Phosphate saline buffer (PBS). The root tips were further mounted on clean grease free slides and observed under a confocal microscope [10].

H_2O_2 content: For quantification of H_2O_2 content from root and shoot tissue, 100mg plant tissue was extracted with 0.1%TCA (Trichloroacetic acid). The reaction mixture contained equal volumes of supernatant and 1M potassium iodide which was followed up with recording the absorbance at 390nm. The H_2O_2 content was determined using the molar extinction coefficient(ε) of 0.28 μM^{-1} cm^{-1} and the concentrations were expressed as µM g^{-1} FW [11].

Histochemical staining for ROS detection: *In situ* localisation of O^{2-} and H_2O_2 in leaves of 21day old seedling of both control and treated sets were performed with the help of Nitro blue tetrazolium (NBT) and 3,3′- diaminobenzidine (DAB) respectively. Fully expanded leaves were collected and immersed in 6mM NBT (dissolved in 10mM sodium citrate buffer pH 6) for detection of O^{2-} accumulation [12]. Furthermore, leaves were incubated in 1mg/ml DAB (dissolved in deionised water pH 3.8 overnight under dark conditions [13]. Further, the leaves were dipped in 80% acetone for complete removal of chlorophyll which was followed by mounting the leaf samples on slides with 20% glycerol for documentation.

Estimation of MDA content: To determine the degree of lipid peroxidation, malondialdehyde (MDA) content was estimated from the plant tissue. 200mg fresh plant tissue was homogenised with 0.1%TCA and the extract was centrifuged following which the supernatant was acquired. The reaction mixture comprising 250ul supernatant with 750ul 20%TCA in 0.5% Thiobarbituric acid (TBA) was incubated in boiling water bath for 30mins. After incubation, the reaction was immediately terminated under cold conditions and the absorbance was recorded at 532nm and 600nm. The MDA content was calculated using the molar extinction coefficient 155.5$mM^{-1}cm^{-1}$ and expressed as µM g^{-1} FW [14].

Methylglyoxal content: Methylglyoxal, a reactive carbonyl species and by-product of photosynthesis as well as respiration was also quantified from fresh plant tissue [15]. The methylglyoxal content was calculated from the standard curve.

Evaluation of Cytotoxicity: Evan's blue, an azo dye which has an intrinsic ability to penetrate through the destabilised membrane of the cells and stain them was utilised for detecting the cell death. To verify the aforementioned parameter, whole root of the rice seedlings was immersed in 0.25% Evan's Blue solution for 10mins. After incubation period, the roots were washed with ddH_2O thoroughly and further dark incubated in N,N-dimethylformamide for 1hr at room temperature. The final absorbance was noted down at 600nm [16]. In-situ detection of cell death was also performed to corroborate the spectrophotometric estimation of cell death with the help of propidium iodide stain. The excised root tips of 21day old rice seedlings were exposed to 8µg/ml PI for 30 mins which was further washed thrice in 1X PBS and observed under confocal microscope (Excitation/ Emission: 587/610nm) [17].

Proline content: For estimation of proline content, 100mg of fresh root and shoot tissue was homogenised in 1ml 0.1M sulphosalicylic acid and the supernatant was collected after centrifugation. The reaction mixture containing 200µl supernatant, 200µl glacial acetic acid and 500µl 2.5% ninhydrin was incubated in boiling water bath for 1hour. After the reaction mixture was cooled down, 900µl toluene was added to terminate the reaction following which the reaction mixture was vortexed and the upper layer was collected for recording the absorbance at 520nm [18].

S1.4. Evaluation of Lignin formation:

Lignin estimation: The lignin content in rice root cell wall was estimated utilising the protocol outlined in reviewed literature with minor modifications [19]. 100mg root tissue was homogenised in 1ml of 95% ethanol which was followed by centrifugation at 4500g for 15

mins. The supernatant was discarded and the pellet was rinsed with 95% ethanol thrice and twice with a solution of n-hexane and 100% ethanol (1:1). The pellet containing the cell wall extract was oven dried at 60ºC and resuspended in 1ml acetylbromide along with 50µl perchloric acid which was incubated for 1hour at 70ºC.The suspended pellet was allowed to cool down followed by addition of 0.9ml 2N NaOH, 0.1ml 7,5M hydroxylamine hydrochloride and centrifuged at 4500g for 5mins. Finally, 0.1 ml supernatant was added to 1ml glacial acetic acid and the absorbance was measured at 280nm. The lignin content was expressed as fold change.

Fluorescent staining of lignin: In-situ localisation of lignin on root cell wall was performed by Auramine-O stain [20]. Root tips were excised and incubated for 10mins in 0.1% Auramine -O stain prepared in 10M Tris-HCl buffer pH (7.4) under dark conditions. The root tips were visualised under a confocal microscope (exc.: 450–490, em.: 515–565 nm).

Determination of cell wall ionically bound GPOD activity: The cell wall ionically bound GPOD activity which is indispensable for lignin polymerisation was analysed as per the procedure proposed by Finger-Teixeira *et al.* [21]. 100mg root tissue was homogenised in 200mM potassium phosphate buffer pH (7.8) containing 0.1mM EDTA. After centrifugation, the supernatant was acquired for soluble GPOD activity estimation and the pellet was dissolved in 1M NaCl followed by incubation at 4ºC up to an hour. The dissolved pellet was re-centrifuged at 2200g for 10mins and the supernatant was collected. The final reaction mixture comprised 10ul supernatant and 990ul 100mM potassium phosphate buffer with 50mM guaiacol and 10mM H_2O_2. The oxidation of guaiacol was noted by an increase in absorbance up to 1min and the enzyme activity was determined using extinction coefficient 26.6$mM^{-1}cm^{-1}$. Root cell wall GPOD activity was expressed as mM product g^{-1} FW min^{-1}.

Determination of PAL activity: Phenylalanine ammonia lyase (PAL) activity was estimated according to the method of Camacho-Gristobal *et al* [22]. 100mg fresh plant samples were homogenised in 1ml extraction buffer comprising 50mM tris-HCl buffer (pH 8) with 2%w/v polyvinylpyrolidone (PVP), 18µM β-mercaptoethanol and 1%v/v TritonX-100 following which the extract was centrifuged at 10,000g for 10mins at 4ºC. 100µl supernatant was added to 540µl Tris-HCl (pH 8) and 200µl 20mM L-phenylalanine. The absorbance of the reaction mixture was recorded immediately at 290nm which was further incubated at 37ºC for 1hour. After incubation, the reaction was terminated by addition of 40µl 5N HCl and the absorbance

was again noted down at 290nm. PAL activity in root tissue was expressed as µM cinnamic acid produced g^{-1} FW min^{-1}.

S1.5. Estimation of enzymatic antioxidant activities:

For analysis of Superoxide dismutase (SOD) (E.C.1.15.1.1), Catalase (CAT, EC 1.11.1.6), Ascorbate peroxidase (APX, EC 1.11.1.11), Guaiacol peroxidase (GPX, 1.11.1.9), Glutathione reductase (GR, EC 1.6.4.2) activities, 200mg fresh plant tissue was extracted in 2ml 200mM potassium phosphate buffer pH 7.8 containing 0.1mM EDTA and centrifuged at 12,000rpm for 15mins under cold conditions [23]. The supernatant was collected for the evaluation of enzymatic antioxidant activities.

SOD activity: To assess Superoxide dismutase (SOD) (E.C.1.15.1.1) activity, 25µl supernatant was added to the reaction mixture consisting of 500µl 80mM tris buffer (pH 8.9) with 0.12mM EDTA, 10.8mM TEMED, 25µl BSA (8.25g/ml), 25 µl 0.6mM Riboflavin (dissolved in 5mM KOH) and 25µl 6mMNBT. The total reaction was exposed to fluorescent light (Philips 40W) for 3mins which led to development of purple coloured solution owing to reduction of NBT into formazan compound. The absorbance of this formazan was read at 560nm and SOD activity was expressed as 50% inhibition in reduction of NBT g^{-1} FW min^{-1}.

CAT activity: Catalase (CAT, EC 1.11.1.6): To the reaction mixture of 975µl 50mM KPO_4 buffer pH 7 and 5µl 20mM H_2O_2, 20µl supernatant was added and the decomposition of H_2O_2 was noted down for 1min at 240nm. The enzyme activity was quantified by the molar extinction coefficient of H_2O_2 (40 mM^{-1} cm^{-1}) and expressed as mM H_2O_2 reduced g^{-1} FW min^{-1}.

APX activity: Ascorbate peroxidase (APX, EC 1.11.1.11): 20µl supernatant was added to the reaction mixture consisting of 970µl 50mM KPO 4 buffer pH 7 with 0.5mM ascorbate and 10µl 0.5mM H_2O_2 This was followed by measuring the absorbance continuously for 1min at 290nm and the enzymatic activity was calculated using the molar extinction coefficient of ascorbate (2.8 mM^{-1} cm^{-1}) and expressed as mM ascorbate decomposed g^{-1} FW min^{-1}.

GPX activity: Guaiacol peroxidase (GPX, 1.11.1.9): To the reaction mixture comprising of 980µl 50mM KPO_4 buffer pH 7 with 50mM guaiacol and 10µl 10mM H_2O_2, 10µl supernatant was added and the increase in absorbance was noted down for 1min at 490nm. GPX activity was estimated using molar extinction coefficient (26.6 mM^{-1} cm^{-1}) and represented as mM product g^{-1} FW min^{-1}.

S1.6. Analysis of non-enzymatic antioxidants:

Reduced glutathione (GSH) content: GSH content was estimated from 21day old seedlings were estimated following the protocol as described by Anderson, [24] with minor modifications. 200mg fresh root and shoot tissue were homogenised in 2ml 5% sulphosalicylic acid and centrifuged at 12,000 rpm for 15mins under cold conditions. For GSH estimation, the final reaction mixture comprising 250µl supernatant, 300µl 0.1M sodium phosphate buffer pH7 with 0.5mM Ethylenediaminetetraacetic acid (EDTA) and 20µl 3mM 5′dithio-bis-2-nitrobenzoic acid (DTNB) was incubated in dark for 5mins. Thereafter, the absorbance was recorded at 412nm and reduced glutathione content was calculated from a standard curve curated from varied concentrations of reduced glutathione.

NPSH content: For total non-protein thiol content (NPSH) quantification, 200mg fresh plant tissue was homogenised in 2ml 5% sulphosalicylic acid and centrifuged to procure the supernatant Del Longo *et al.* [25]. 250µl supernatant was added to 1ml 150mM sodium phosphate buffer pH7.4 containing 5mM EDTA and 500µl 6mM DTNB. The reaction mixture was incubated under dark conditions for 30mins and the absorbance was recorded at 412nm. The NPSH content was estimated from a standard curve prepared from varying concentrations of cysteine. Phytochelatin contents were determined by calculating the difference between NPSH and GSH contents Bhargava *et al.* [26].

Cysteine content: For analysing the cysteine content, a precursor molecule for GSH biosynthetic pathway fresh root and shoot tissues were homogenised in 5% perchloric acid under cold conditions. Following centrifugation, 200µl supernatant was added to 1ml freshly prepared acid ninhydrin and incubated in water bath at 70ºC for 30mins. The absorbance was recorded at 560nm and the cysteine concentration extrapolated using the standard curve of cysteine was expressed as mM g^{-1} FW [27].

Estimation of Ascorbate contents: Reduced ascorbate (AsA) and total ascorbate contents were estimated according to the protocol described by Cakmak and Marschner, [28]. 200mg fresh root and shoot tissue were homogenised in 2ml 75mM sodium phosphate buffer following which centrifugation was performed to collect the supernatant. For total ascorbate content estimation, the reaction mixture with 200µl supernatant, 250µl 150mM sodium phosphate buffer (pH 7.4) containing 5mM EDTA, 50µl 10mM DTT, 50µl 0.5% N-ethylmaleimide (NEM), 10% 200µl TCA, 200µl 44% orthophosphoric acid, 200µl 4% α-2,1 bipyridine and 200µl 3% $FeCl_3$ was incubated in water bath at 40ºC for 40mins. In reduced ascorbate content estimation, the

reaction mixture comprising 200µl supernatant, 250µl 150mM sodium phosphate buffer (pH 7.4) containing 5mM EDTA, 100µl H_2O, 200µl 10%TCA, 200µl 44% orthophosphoric acid, 200µl 4% α-2,1 bipyridine and 200µl 3% $FeCl_3$ was incubated for same duration and temperature in water bath. The absorbance for both the reactions was recorded at 525nm and the contents were calculated from a standard curve prepared using ascorbic acid. The total and oxidised ascorbate contents were represented as mM ascorbate gm^{-1} FW.

S1.7. Analysis of secondary metabolites:

Total phenol content was analysed using Folin-ciocalteau reagent where fresh root and shoot samples were extracted with 80% ethanol. The final reaction mixture comprised of 150µl supernatant, 250µl 10% Folin-ciocalteau reagent and 300µl 20% sodium carbonate (Na_2CO_3) which was incubated under dark conditions for 30mins at room temperature. The absorbance was noted down at 765nm and the total Phenol Content was expressed mg gallic acid (GAE)/ Equivalent gm of tissue [29].

Total flavonoid content was estimated from fresh root and shoot samples by homogenising them in 80% ethanol. After centrifugation, 100µl supernatant was added to 500µl 80% ethanol and this reaction mixture was incubated for 5mins. This was followed up by addition of 100µl 10% $AlCl_3$, 100µl 6% $NaNO_2$ and 500µl 1N NaOH. This reaction mixture was further incubated up to 30mins at room temperature and the absorbance was read at 510nm. The total flavonoid content was calculated from a standard curve prepared using quercetin and the estimated values were expressed as mg gm^{-1} FW [30].

S1.8. Statistical analysis:

All experiments were performed in triplicates (n=3) and mean values of triplicate data were plotted as a histogram. Further, for data analysis of detailed experimental study One-way analysis of variance (ANOVA) was performed by Tukey's HSD multiple comparison test ($p < 0.05$) was performed to confirm the significance of procured data. All Graphs were prepared by GraphPad Prism 8.02.263.

S2. Results:

S2.1. Selection of optimum concentration of Bimetallic Nanoparticles (BNPs) for Cd remediation:

25mg L^{-1} Fe-ZnBNP emerged to be an appropriate concentration for amelioration of Cd stress in 21days old rice seedlings in terms of enhanced growth parameters including root and shoot length as well as RWC% (Fig.S1A-E). Moreover, this optimum dosage of BNP was also efficient in restoring the photosynthetic pigment levels which were drastically hampered on exposure to 10µM $CdCl_2$ stress. It was observed that 50mg L^{-1} Fe-ZnBNP was showing phytotoxic effects on plant since certain NPs tend to exhibit toxic effects when applied at a supra-optimal level[31]. Evidently, co-application of 10µM $CdCl_2$ and 50mg L^{-1} Fe-ZnBNP documented reduced growth, RWC% and chlorophyll contents.

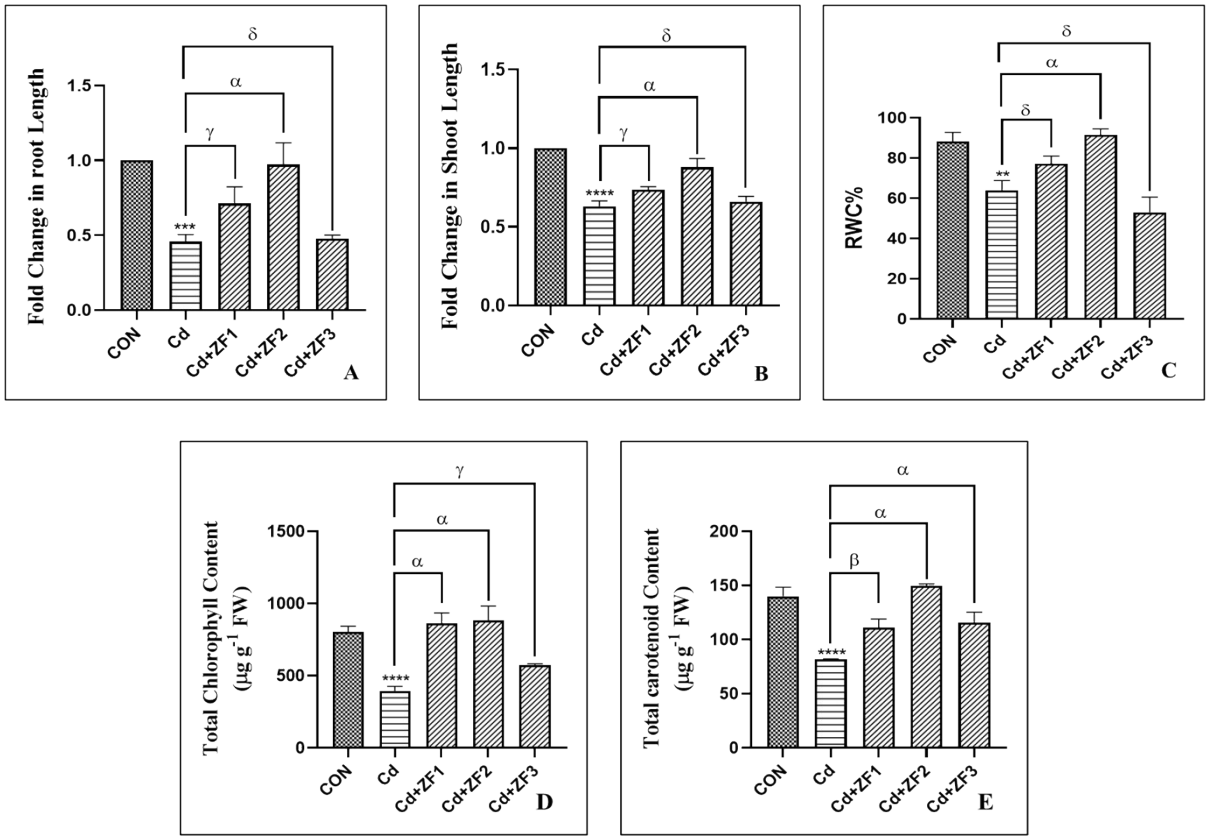

Fig.S1. Selection of an optimum dosage of Fe-ZnBNPs for amelioration of Cd on basis of growth parameters, RWC% and photosynthetic pigment content A) Root Length; B) Shoot Length; C) RWC%; D) Total Chlorophyll content; E) Carotenoid content. The Stars denote significant statistical difference at $p<0.05$; ns: $P > 0.05$, *: $P \leq 0.05$, **: $P \leq 0.01$, ****: $P \leq 0.001$ and indicates difference between control and Cd. Symbols denote significant differences between Cd and Cd+ZF1, Cd+ZF2, Cd+ZF3 treatments; δ: P > 0.0 5, γ: $P \leq 0.05$, β: $P \leq 0.01$, α : $P \leq 0.001$.

[CON (0 Cd+0Fe-ZnBNP), Cd (10µM $CdCl_2$), Cd+ZF1 (10µM $CdCl_2$+ 10mg L^{-1} Fe-ZnBNP), Cd+ZF2 (10µM $CdCl_2$+ 25mg L^{-1} Fe-ZnBNP), Cd+ZF3 (10µM $CdCl_2$+ 50mg L^{-1} Fe-ZnBNP)]

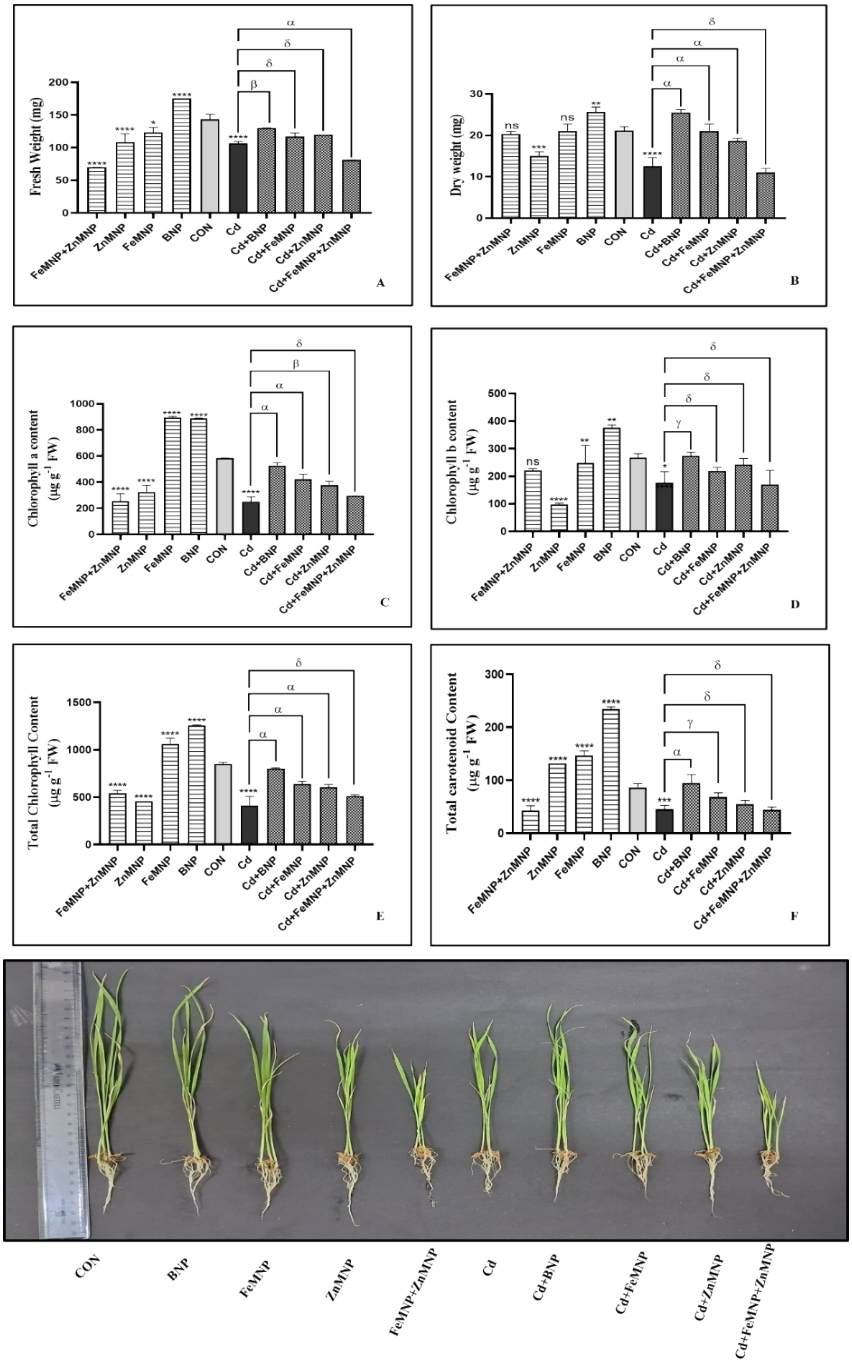

Fig.S2. Comparative analysis of Fe-ZnBNP, Fe_3O_4 MNP and ZnO MNP on growth parameters and photosynthetic pigment contents A) Fresh Weight; B) Dry Weight; C) Chlorophyll a content; D) Chlorophyll b content; E) Total Chlorophyll content; F) Carotenoid content, G) Phenotypic characters of the seedlings. The Stars denote significant statistical difference at $p<0.05$; ns: $P > 0.05$, *: $P \leq 0.05$, **: $P \leq 0.01$, ****: $P \leq 0.001$ and indicates difference between control and Cd, Fe-ZnBNP, FeMNP, ZnMNP, FeMNP+ZnMNP; Symbols denote significant differences between Cd and Cd+BNP, Cd+FeMNP, Cd+ZnMNP, Cd+FeMNP+ZnMNP treatments; δ: P > 0.0 5, γ: $P \leq 0.05$, β: $P \leq 0.01$, α : $P \leq 0.001$.

[CON (0 Cd+0Fe-ZnBNP), BNP (25 mg L^{-1} Fe-ZnBNP), FeMNP (25 mg L^{-1} Fe_3O_4MNP), ZnMNP (25 mg L^{-1} ZnOMNP), FeMNP+ZnMNP (25 mg L^{-1} Fe_3O_4MNP+ZnOMNP), Cd (10µM $CdCl_2$), Cd+BNP (10µM $CdCl_2$+ 25 mg L^{-1} Fe-ZnBNP), Cd+FeMNP (10µM $CdCl_2$+ 25 mg L^{-1} Fe_3O_4MNP), Cd+ZnMNP (10µM $CdCl_2$+ 25 mg L^{-1} ZnOMNP), Cd+FeMNP+ZnMNP (10µM $CdCl_2$+ 25 mg L^{-1} Fe_3O_4MNP+ZnOMNP)]

S2.3. Fe-ZnBNP on C assimilation:

This study indicated a significant alteration in reducing sugar content when seedlings were subjected to Cd singly or simultaneously treated with Cd and Fe-ZnBNP (Fig.S3A, B). It was documented that reducing sugar was significantly high in shoot and less in root in seedlings treated with Cd only whereas reciprocal levels were observed in shoot and root when supplemented with BNP. Meanwhile the non -reducing sugar content was significantly elevated under Cd stress in 21days old rice seedlings indicating its role as an osmolyte (Fig.S3C, D). Co-application of Cd and Fe-ZnBNP notably reduced the non-reducing sugar levels in both root and shoot tissues. Individual supplementation of Fe-ZnBNP decreased the reducing sugar contents albeit it amplified the non -reducing sugar contents in both root and shoot of 21days old seedlings.

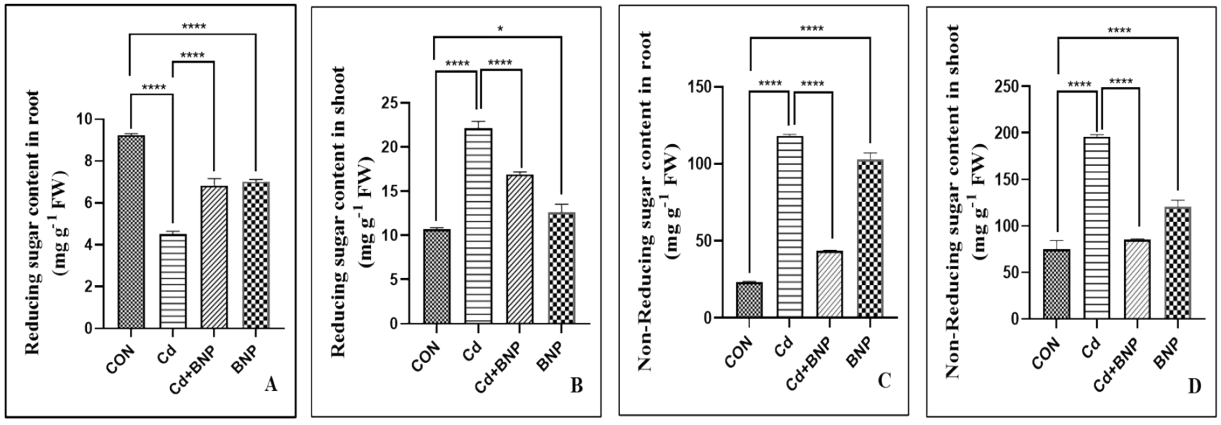

Fig.S3. Analysis of sugar content in 21days old seedlings post treatment with Fe-ZnBNP. A) Reducing Sugar Content in root; B) Reducing Sugar Content in Shoot; C) Non-Reducing Sugar content in root; D) Non-Reducing Sugar content in Shoot. The data represent the mean values of three replicates and the bars represent standard deviations. The Stars denote significant statistical difference at $p<0.05$; ns: $P>0.05$, *: $P \leq 0.05$, **: $P \leq 0.01$, ***: $P \leq 0.001$.

[CON (0 Cd+0Fe-ZnBNP), Cd (10 µM $CdCl_2$), Cd+BNP (10 µM $CdCl_2$+ 25 mg L^{-1} Fe-ZnBNP), BNP (25 mg L^{-1} Fe-ZnBNP)]

S2.4. Fe-ZnBNP altered the severe morphological anomalies induced by Cd:

SEM micrographs of the root tips and stomata revealed extensive morphological aberrations in 21days old seedlings exposed solely to Cd. Cd treatment caused extensive distortions in the guard cells as observed (Fig.S4) along with inhibition in optimum stomatal opening. Cd also induced loosening of epidermal tissue eventually leading to tearing and created notable breaks at the root tips. However, supplementation of Fe-ZnBNP to Cd treated seedlings subsequently restored the morphology as well as facilitated the opening of stomata. Fe-ZnBNP also restored the normal integrity of epidermal root tissue and exhibited an intact root surface.

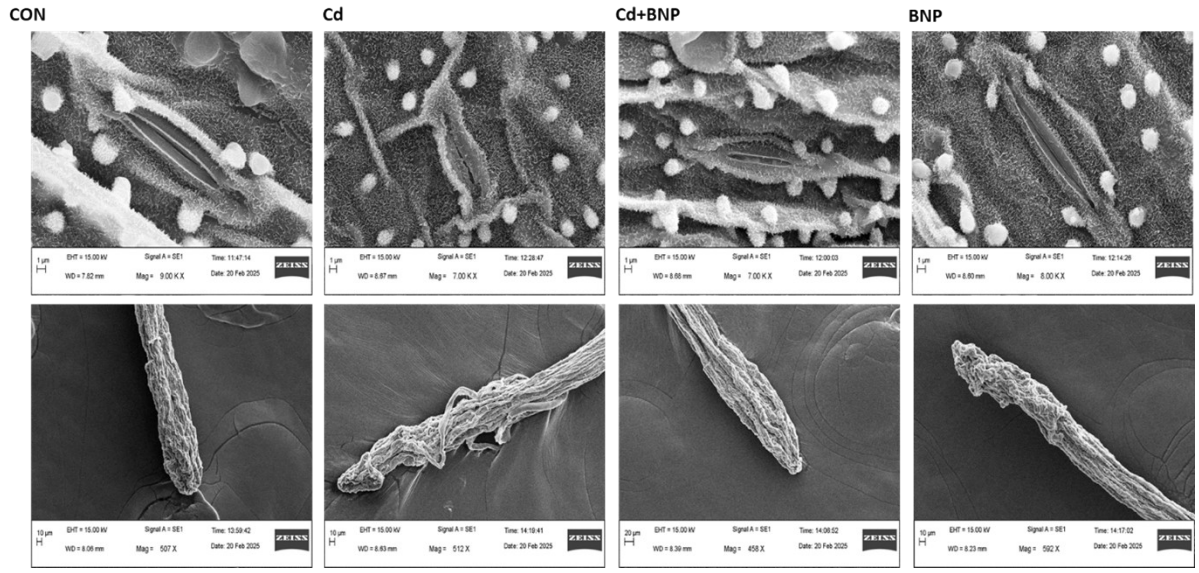

Fig.S4. Scanning electron micrograph (SEM) of Stomata and root tips of 21days old rice seedlings under co-application of Cd and Fe-ZnBNP and individual application of Fe-ZnBNP.

[CON (0 Cd+0Fe-ZnBNP), Cd (10 µM $CdCl_2$), Cd+BNP (10 µM $CdCl_2$+ 25 mg L^{-1} Fe-ZnBNP), BNP (25 mg L^{-1} Fe-ZnBNP)

S2.5. Analysis of oxidative stress parameters:

Cd treated seedlings vividly denoted the overproduction of H_2O_2 by 48.65% and 43.16% in root and shoot respectively in comparison to control seedlings. On the contrary to Cd affected seedlings, application of Fe-ZnBNP imparted a significant drop in the endogenous H_2O_2 content in both root and shoot by 78.17% and 35.12% respectively (Fig.S5A, B). Solitary supplementation of Fe-ZnBNP significantly reduced the H_2O_2 formation in root and shoot of 21days old seedlings which clearly elucidated that BNP application did not generate any oxidative stress.

Accumulation of proline in root and shoot clearly indicates activation of stress tolerance mechanism in plants in response to abiotic and biotic stress factors which eventually deters membrane instability and maintains redox homeostasis. There was a significant increase in proline content in root (81.95%) and shoot (79.98%) of seedlings subjected to Cd toxicity in comparison to control seedlings to maintain the redox homeostasis in response to exorbitant oxidative stress induced by Cd. However, in BNP supplemented seedlings a significant reduction in proline content was observed in root by 63.90% and in shoot by 61.84% contrarily to seedlings treated alone with Cd (Fig.S5C, D). Individual supplementation of BNP notably increased the proline content in root and shoot of 21days old seedlings.

Methylglyoxal, an α-oxoaldehyde and cytotoxic byproduct of several crucial metabolic pathways is also considered to be a hallmark of heavy metal stress as their escalated content is associated with perpetuation of redox homeostasis along with glyoxalase [32]. A similar trend of increase in methylglyoxal levels was observed in root and shoot of Cd treated seedlings where the increment percentage was 75.22 and 52.40 respectively (Fig.S5E, F). The ameliorative potential of Fe-ZnBNP was reflected when Cd treated seedlings supplemented with the BNP remarkably reduced the methylglyoxal formation by 83.25% (root) and 25.44% (shoot) in contrast to seedlings entirely exposed to Cd.

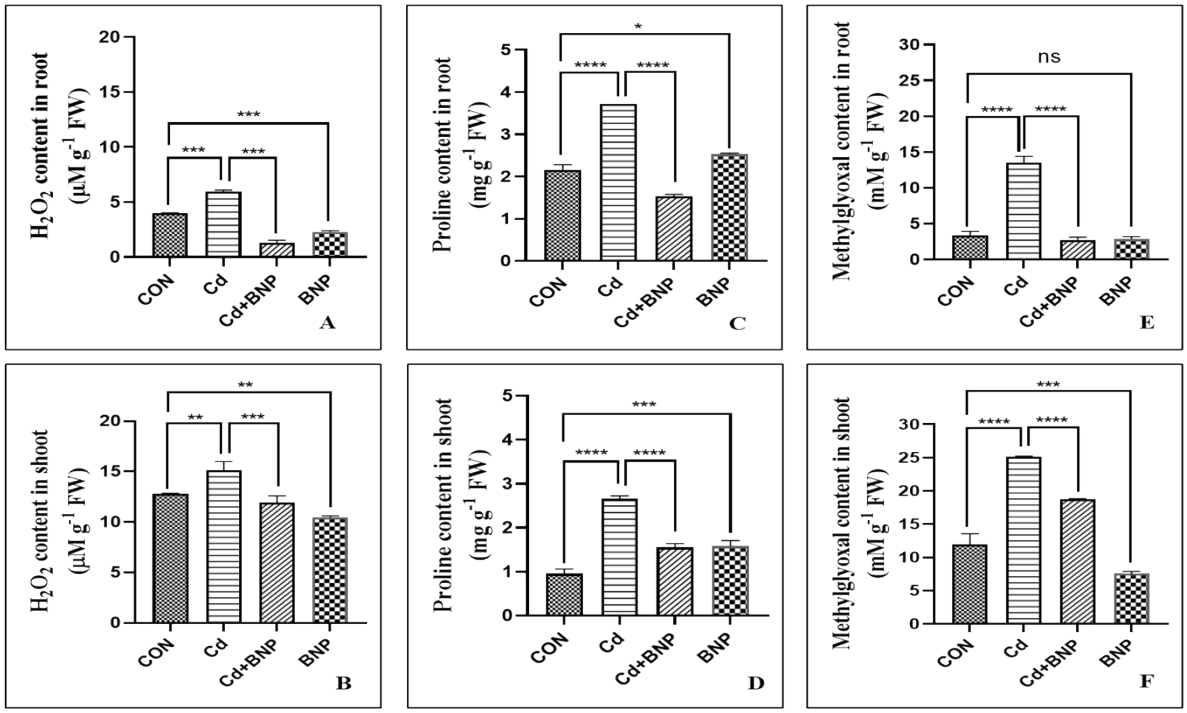

Fig.S5. Evaluation of stress parameters in 21days old seedlings post co-treatment with Cd and Fe-ZnBNP. A) H_2O_2 Content in root; B) H_2O_2 Content in Shoot; C) Proline content in root; D)

Proline content in Shoot E) Methylglyoxal content in root F) Methylglyoxal content in Shoot. The data represent the mean values of three replicates and the bars represent standard deviations. The Stars denote significant statistical difference at $p<0.05$; ns: $P>0.05$, *: $P \leq 0.05$, **: $P \leq 0.01$, ***: $P \leq 0.001$.

[CON (0 Cd+0Fe-ZnBNP), Cd (10 μM $CdCl_2$), Cd+BNP (10 μM $CdCl_2$+ 25 mg L^{-1} Fe-ZnBNP), BNP (25 mg L^{-1} Fe-ZnBNP)]

S2.6. Regulation of oxidative stress by non-enzymatic anti-oxidant activities:

Non-enzymatic antioxidants were also estimated in terms of reduced ascorbate and total ascorbate content. The data revealed how rice seedlings subjected to Cd toxicity compromised AsA accumulation in the root whereas Cd significantly elevated the AsA content in the shoot comparative to untreated seedlings. However, co-application of Cd and Fe-ZnBNP was documented with the maximum amount of AsA accumulation in the root tissue accounting to 79.31% higher than Cd treated seedlings (Fig.S6A, B). Fe-ZnBNP supplementation profoundly lowered the AsA content in the shoot by 31.74% conversely to seedlings subjected entirely to Cd stress. Exposure to Cd elicited radical accumulation of the total ascorbate in both root as well as shoot tissue of the 21days old seedlings by 58.55% and 29.31% respectively comparative to untreated seedlings. Meanwhile, supplementation of Fe-ZnBNP to Cd treated seedlings was reported to possess lower total ascorbate content in the roots despite a significant enhancement in the content in shoot which apparently imparts resilience towards Cd inflicted oxidative stress (Fig.S6C, D).

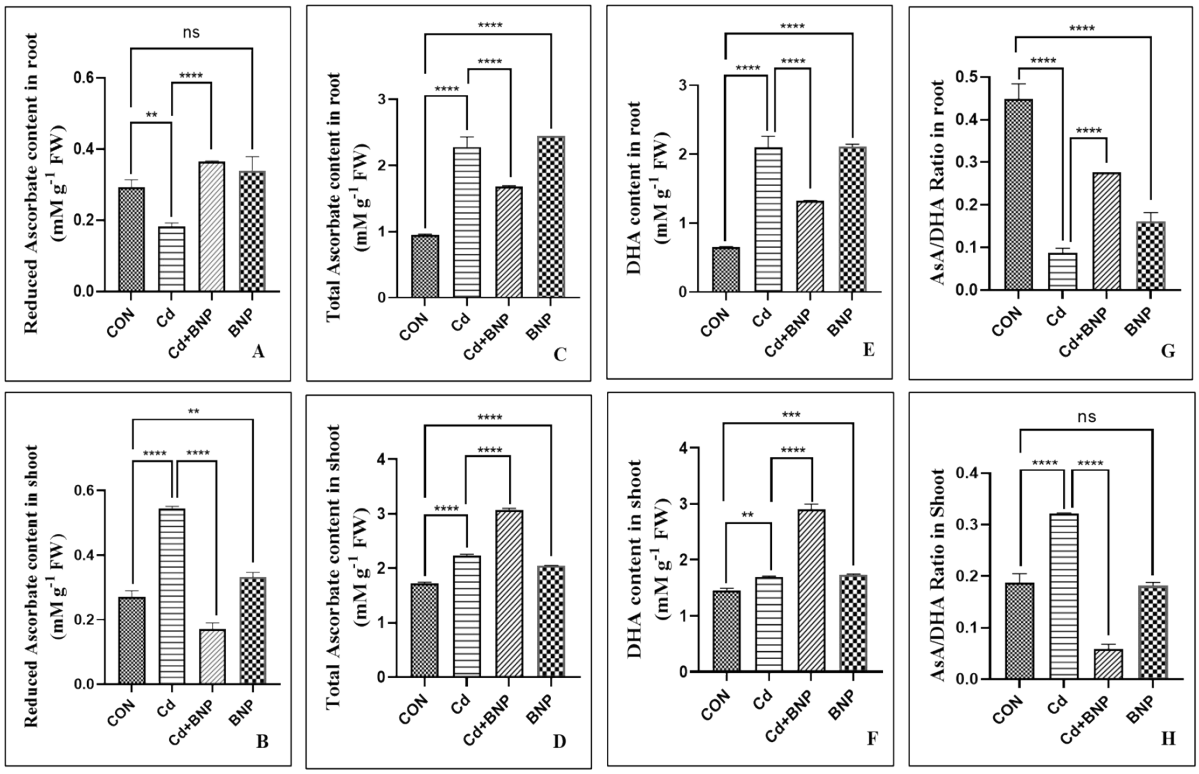

Fig.S6. Evaluation of ascorbate metabolism in 21days old seedlings post co-treatment with Cd and Fe-ZnBNP. A) Reduced Ascorbate (AsA) Content in root; B) Reduced Ascorbate Content (AsA) in Shoot; C) Total Ascorbate content in root; D) Total Ascorbate content in Shoot E) Dehydroascorbate (DHA) content in root F) Dehydroascorbate (DHA) content in Shoot G) AsA/DHA Ratio in root H) AsA/DHA Ratio in Shoot. The data represent the mean values of three replicates and the bars represent standard deviations. The Stars denote significant statistical difference at $p<0.05$; ns: $P>0.05$, *: $P \leq 0.05$, **: $P \leq 0.01$, ***: $P \leq 0.001$.

[CON (0 Cd+0Fe-ZnBNP), Cd (10 µM $CdCl_2$), Cd+BNP (10 µM $CdCl_2$+ 25 mg L^{-1} Fe-ZnBNP), BNP (25 mg L^{-1} Fe-ZnBNP)]

S2.7. Effect on secondary metabolites:

The total flavonoid and phenol contents as analysed from 21days old Cd treated seedlings recorded a similar trend of increase in contrary to the control seedlings (Fig.S7A-D). The total flavonoid content spiked to 63.221% in root and 42.80% in shoot in response to Cd stress. Meanwhile, the total phenol content was escalated by 22.65% in root and 25.95% in shoot of seedlings subjected to Cd toxicity which attributed to the significant increment in the PAL activity of the seedlings. Contrarily to only Cd treated set, co- application of Cd and Fe-ZnBNP significantly decreased the flavonoid content by 74.80% in root and 47.33% in shoot. Furthermore, the total phenolic content also reduced likewise flavonoid content in root by

25.34% and shoot by 13.424% on co-application of Cd and Fe-ZnBNP comparative to seedlings solely subjected to detrimental effects of Cd.

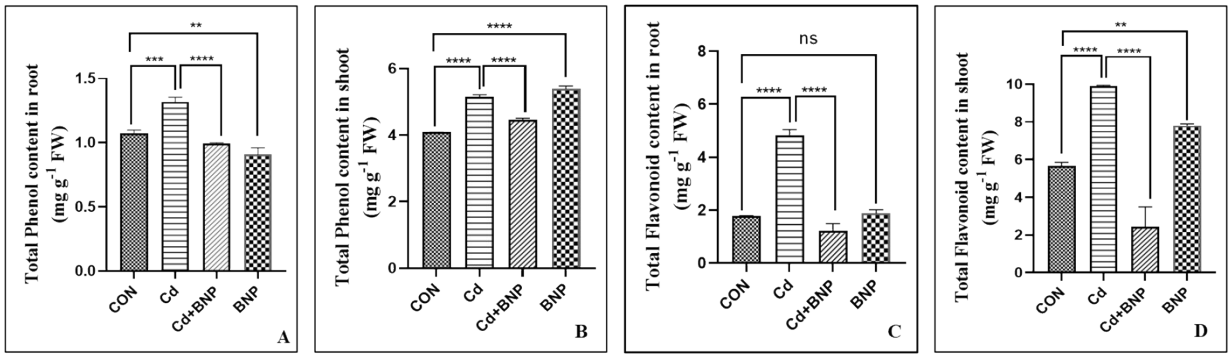

Fig.S7. Evaluation of secondary metabolites in 21days old seedlings post co-treatment with Cd and Fe-ZnBNP. A) Total Phenol Content in root; B) Total Phenol Content in Shoot; C) Total Flavonoid content in root; D) Total Flavonoid content in Shoot. The data represent the mean values of three replicates and the bars represent standard deviations. The Stars denote significant statistical difference at $p<0.05$; ns: $P>0.05$, *: $P \leq 0.05$, **: $P \leq 0.01$, ***: $P \leq 0.001$.

[CON (0 Cd+0Fe-ZnBNP), Cd (10 µM $CdCl_2$), Cd+BNP (10 µM $CdCl_2$+ 25 mg L^{-1} Fe-ZnBNP), BNP (25 mg L^{-1} Fe-ZnBNP)]

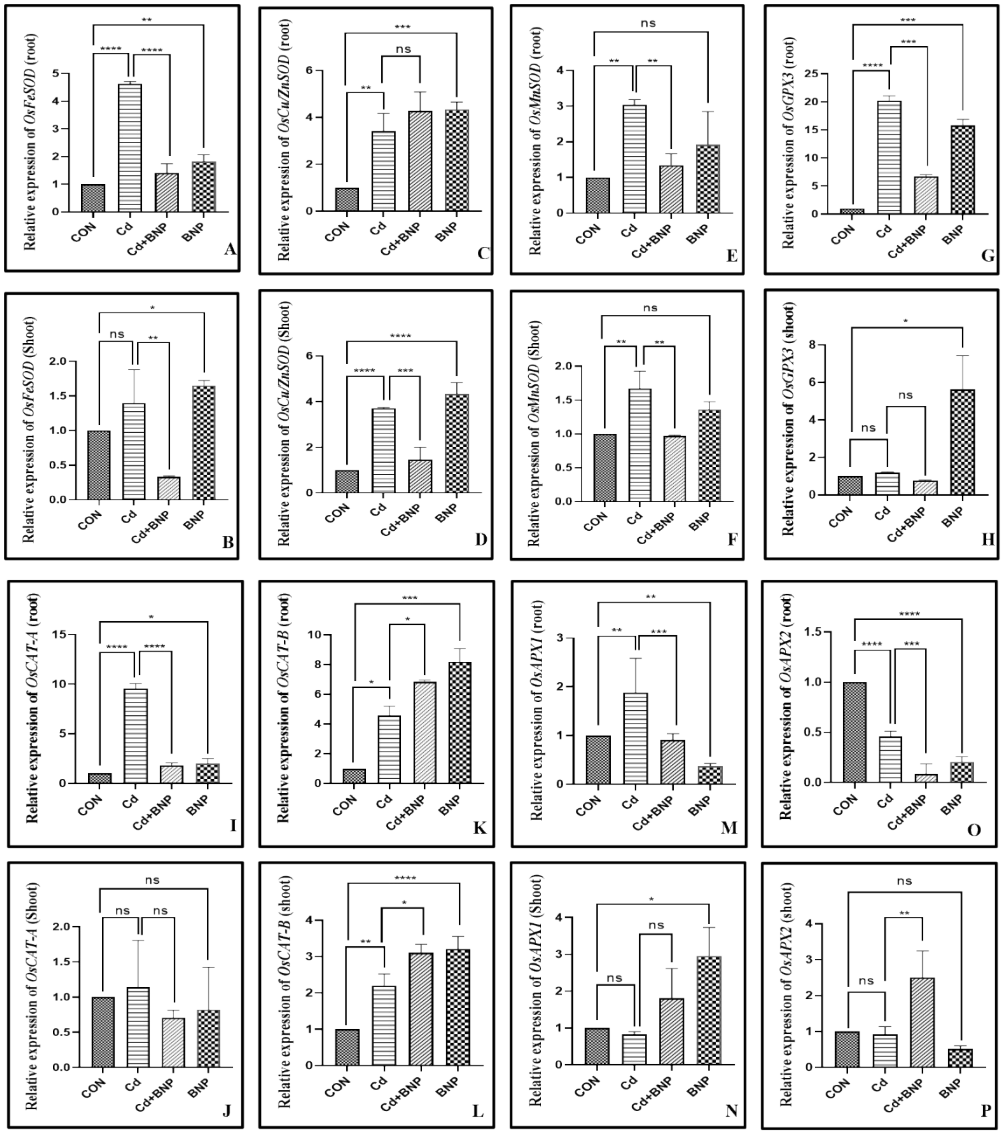

Fig.S8. Relative expression of A) *OsFeSOD* in root; B) *OsFeSOD* in shoot; C) *OsCu/ZnSOD* in root; D) *OsCu/ZnSOD* in shoot; E) *OsMnSOD* in root; F) *OsMnSOD* in shoot; G) *OsGPX3* in root; H) *OsGPX3* in shoot; I) *OsCAT-A* in root; J) *OsCAT-A* in shoot; K) *OsCAT-B* in root; L) *OsCAT-B* in shoot; M) *OsAPX-1* in root; N) *OsAPX-1* in shoot; O) *OsAPX-2* in root; P) *OsAPX2* in shoot. The data represent the mean values of three replicates and the bars represent standard deviations. The Stars denote significant statistical difference at $p<0.05$; ns: $P>0.05$, *: $P \leq 0.05$, **: $P \leq 0.01$, ***: $P \leq 0.001$.

[CON (0 Cd+0Fe-ZnBNP), Cd (10 µM $CdCl_2$), Cd+BNP (10 µM $CdCl_2$+ 25 mg L^{-1} Fe-ZnBNP), BNP (25 mg L^{-1} Fe-ZnBNP)]

Table S1: List of primer sequences:

Gene		5′ to 3′ sequences
OsZIP1	Forward	5′- TGCGCCCATGTATGTATGCT -3′
	Reverse	5′- CATGAACTGTTTCGGCCACG -3′
OsZIP4	Forward	5′- CGATCTCCTCGCTGCAGATT -3′
	Reverse	5′- GCCCATATGGCAAGCAGAGA -3′
OsIRT1	Forward	5′- CGTCTTCTTCTTCTCCACCACGA -3′
	Reverse	5′- GCAGCTGATCGAGTCTGACC -3′
OsPCS1	Forward	5′- AGGTCCTACAGCAAATCCGT -3′
	Reverse	5′- ATTCCCACTTAGCAATGCGG -3′
OsHMA3	Forward	5′- GTTCAGCATCGACTCGTTCG -3′
	Reverse	5′- CCACATTTTCCGGGTTTGGT -3′
OsCATA	Forward	5′- GTGAAGATTGCGAATAGGCTC-3′
	Reverse	5′- TCTGGCCTTATTTGGTTGGT-3′
OsCATB	Forward	5′- GACAAGGAGAACAATTTCCAACAG-3′
	Reverse	5′- AGTAGGAGATCCAGATGCCAC-3′
OsMnSOD	Forward	5′- ATAACCTCAAGCCTATCAGCG-3′
	Reverse	5′- ACCCATCCAGATCCTTGTAAAG-3′
OsFeSOD	Forward	5′- CAAGTCACAAACCCAGAGTCAT-3′
	Reverse	5′- GGAATACAAGATGTCAGGCTCA-3′
OsCu/ZnSOD	Forward	5′- GCTCTATTGCGTTGTATGCCA-3′
	Reverse	5′- GCTTGACTCCCAAATGGTGAC-3′
OsAPX1	Forward	5′- TCAGGACATTGTTGCCCTC-3′
	Reverse	5′- GTCACCACTCAGAAGCTCC-3′
OsAPX2	Forward	5′- CTCTCCTACGCCGACTTCTAC-3′
	Reverse	5′- AGGTGGTCAGAACCTTGTGT-3′
OsGPX3	Forward	5′- TTGCATTGAGCACTTGGAAC-3′
	Reverse	5′- AGGGGCAAAGTGATGCAGTA-3′
GAPDH	Forward	5′- AAGCCAGCATCCTATGATCAGATT -3′
	Reverse	5′- CGTAACCCAGAATACCCTTGAGTTT -3′

References:

1. Lichtenthaler HK. [34] Chlorophylls and carotenoids: pigments of photosynthetic biomembranes. *InMethods in enzymology* 1987 Jan 1 (Vol. 148, pp. 350-382). Academic Press. doi.org/10.1016/0076-6879(87)48036-1
2. Masoner M, Kasemir H. Control of chlorophyll synthesis by phytochrome: I. The effect of phytochrome on the formation of 5-aminolevulinate in mustard seedlings. *Planta*. 1975 Jan;126(2):111-7. doi.org/10.1007/BF00380614
3. Bogorad LJ. [122] Porphyrin synthesis. *InMethods in enzymology* 1962 Jan 1 (Vol. 5, pp. 885-895). Academic Press. doi.org/10.1016/S0076-6879(62)05334-3

4. Hu G, Zhou X, Chao M, Hu H. Roles of Exogenous 5-Aminolevulinic Acid and Dihydroporphyrin Iron in Chlorophyll Precursor Synthesis and Chlorophyll-Related Enzyme Activities in Wheat Under Different Light Intensities. *Agronomy*. 2024 Oct 22;14(11):2464. **doi.org/10.3390/agronomy14112464**
5. Bauer H, Senser M. Photosynthesis of ivy leaves (Hedera helix L.) after heat stress II. Activity of ribulose bisphosphate carboxylase, Hill reaction, and chloroplast ultrastructure. Zeitschrift für Pflanzenphysiologie. 1979 Mar 1;91(4):359-69. doi.org/10.1016/S0044-328X(79)80047-1
6. DuBois M, Gilles KA, Hamilton JK, Rebers PA, Smith F. Colorimetric method for determination of sugars and related substances. *Analytical chemistry*. 1956 Mar 1;28(3):350-6.
7. Miller GL. Estimation of reducing sugar by dinitrosalicylic acid method. *Anal. Chem*. 1972;31:426-8.
8. Barman F, Guha T, Kundu R. Exogenous Selenium Supplements Reduce Cadmium Accumulation and Restore Micronutrient Content in Rice Grains. *Journal of Soil Science and Plant Nutrition*. 2025 Feb 10:1-9.doi.org/10.1007/s42729-025-02267-5
9. Jambunathan N. Determination and detection of reactive oxygen species (ROS), lipid peroxidation, and electrolyte leakage in plants. *Plant stress tolerance*: *methods and protocols*. 2010:291-7. doi.org/10.1007/978-1-60761-702-0_18
10. Das A, Pal S, Chakraborty N, Hasanuzzaman M, Adak MK. Regulation of reactive oxygen species metabolism and oxidative stress signaling by abscisic acid pretreatment in rice (Oryza sativa L.) seedlings through sub1A QTL under salinity. *Plant Stress*. 2024 Mar 1;11:100422. doi.org/10.1016/j.stress.2024.100422
11. Velikova V, Yordanov I, Edreva AJ. Oxidative stress and some antioxidant systems in acid rain-treated bean plants: protective role of exogenous polyamines. *Plant science*. 2000 Feb 7;151(1):59-66. doi.org/10.1016/S0168-9452(99)00197-1
12. Fryer MJ, Oxborough K, Mullineaux PM, Baker NR. Imaging of photo-oxidative stress responses in leaves. *Journal of experimental botany*. 2002 May 15;53(372):1249-54. doi.org/10.1093/jexbot/53.372.1249
13. Thordal-Christensen H, Zhang Z, Wei Y, Collinge DB. Subcellular localization of H2O2 in plants. H2O2 accumulation in papillae and hypersensitive response during the barley—powdery mildew interaction. *The Plant Journal*. 1997 Dec;11(6):1187-94. **doi.org/10.1046/j.1365-313X.1997.11061187.x**

14. Heath RL, Packer L. Photoperoxidation in isolated chloroplasts: I. Kinetics and stoichiometry of fatty acid peroxidation. *Archives of biochemistry and biophysics*. 1968 Apr 1;125(1):189-98. doi.org/10.1016/0003-9861(68)90654-1
15. Wild R, Ooi L, Srikanth V, Münch G. A quick, convenient and economical method for the reliable determination of methylglyoxal in millimolar concentrations: the N-acetyl-L-cysteine assay. *Analytical and Bioanalytical Chemistry*. 2012 Jul;403:2577-81. doi.org/10.1007/s00216-012-6086-4
16. Jacyn Baker C, Mock NM. An improved method for monitoring cell death in cell suspension and leaf disc assays using Evans blue. Plant Cell, Tissue and Organ Culture. 1994 Oct;39:7-12. doi.org/10.1007/BF00037585
17. Liu J, Lv Y, Li M, Wu Y, Li B, Wang C, Tao Q. Peroxidase in plant defense: Novel insights for cadmium accumulation in rice (Oryza sativa L.). *Journal of Hazardous Materials*. 2024 Aug 5;474:134826 doi.org/10.1016/j.jhazmat.2024.134826
18. Bates LS, Waldren RP, Teare ID. Rapid determination of free proline for water-stress studies. *Plant and soil*. 1973 Aug;39:205-7. doi.org/10.1007/BF00018060
19. Rui H, Chen C, Zhang X, Shen Z, Zhang F. Cd-induced oxidative stress and lignification in the roots of two Vicia sativa L. varieties with different Cd tolerances. *Journal of Hazardous Materials*. 2016 Jan 15;301:304-13. doi.org/10.1016/j.jhazmat.2015.08.052
20. Molnár Á, Rónavári A, Bélteky P, Szőllősi R, Valyon E, Oláh D, Rázga Z, Ördög A, Kónya Z, Kolbert Z. ZnO nanoparticles induce cell wall remodeling and modify ROS/RNS signalling in roots of Brassica seedlings. *Ecotoxicology and Environmental Safety*. 2020 Dec 15;206:111158. doi.org/10.1016/j.ecoenv.2020.111158
21. Finger-Teixeira A, Ferrarese MD, Soares AR, da Silva D, Ferrarese-Filho O. Cadmium-induced lignification restricts soybean root growth. *Ecotoxicology and Environmental Safety*. 2010 Nov 1;73(8):1959-64. doi.org/10.1016/j.ecoenv.2010.08.021
22. Camacho-Cristóbal JJ, Anzellotti D, González-Fontes A. Changes in phenolic metabolism of tobacco plants during short-term boron deficiency. *Plant Physiology and Biochemistry*. 2002 Dec 1;40(12):997-1002. doi.org/10.1016/S0981-9428(02)01463-8
23. Dey S, Kundu R, Gopal G, Mukherjee A, Nag A, Paul S. Enhancement of nitrogen assimilation and photosynthetic efficiency by novel iron pulsing technique in Oryza

sativa L. var Pankaj. *Plant Physiology and Biochemistry*. 2019 Nov 1;144:207-21. doi.org/10.1016/j.plaphy.2019.09.037

24. Anderson ME. [70] Determination of glutathione and glutathione disulfide in biological samples. *InMethods in enzymology* 1985 Jan 1 (Vol. 113, pp. 548-555). Academic Press. doi.org/10.1016/S0076-6879(85)13073-9
25. Del Longo OT, González CA, Pastori GM, Trippi VS. Antioxidant defences under hyperoxygenic and hyperosmotic conditions in leaves of two lines of maize with differential sensitivity to drought. *Plant and cell physiology*. 1993 Oct 1;34(7):1023-8. doi.org/10.1093/oxfordjournals.pcp.a078515
26. Bhargava P, Srivastava AK, Urmil S, Rai LC. Phytochelatin plays a role in UV-B tolerance in N2-fixing cyanobacterium Anabaena doliolum. *Journal of Plant Physiology*. 2005 Nov 15;162(11):1220-5. doi.org/10.1016/j.jplph.2004.12.006
27. Gaitonde MK. A spectrophotometric method for the direct determination of cysteine in the presence of other naturally occurring amino acids. *Biochemical Journal*. 1967 Aug;104(2):627. doi: 10.1042/bj1040627
28. Cakmak I, Marschner H. Magnesium deficiency and high light intensity enhance activities of superoxide dismutase, ascorbate peroxidase, and glutathione reductase in bean leaves. *Plant physiology*. 1992 Apr 1;98(4):1222-7. doi.org/10.1104/pp.98.4.1222
29. Kaur R, Arora S, Singh B. Antioxidant activity of the phenol rich fractions of leaves of Chukrasia tabularis A. Juss. *Bioresource technology*. 2008 Nov 1;99(16):7692-8. doi.org/10.1016/j.biortech.2008.01.070
30. Ibrahim MH, Jaafar HZ, Rahmat A, Rahman ZA. Involvement of nitrogen on flavonoids, glutathione, anthocyanin, ascorbic acid and antioxidant activities of Malaysian medicinal plant Labisia pumila Blume (Kacip Fatimah). *International Journal of Molecular Sciences*. 2011 Dec 29;13(1):393-408. **doi.org/10.3390/ijms13010393**
31. Muzammil S, Ashraf A, Siddique MH, Aslam B, Rasul I, Abbas R, Afzal M, Faisal M, Hayat S. A review on toxicity of nanomaterials in agriculture: Current scenario and future prospects. *Science Progress*. 2023 Oct;106(4):00368504231221672. doi: 10.1177/00368504231221672
32. Zheng Q, Xin J, Zhao C, Tian R. Role of methylglyoxal and glyoxalase in the regulation of plant response to heavy metal stress. *Plant Cell Reports*. 2024 Apr;43(4):103. DOI: doi.org/10.1007/s00299-024-03186-y